Environ Earth Sci (2016) 75:636
DOI 10.1007/s12665-016-5445-4

ORIGINAL ARTICLE

Determination of the origins and recharge rates of the Sfax aquifer system (southeastern Tunisia) using isotope tracers

Rahma Ayadi[1,2] · Kamel Zouari[1] · Hakim Saibi[2] · Rim Trabelsi[1] · Hafedh Khanfir[3] · Ryuichi Itoi[2]

Received: 15 July 2015 / Accepted: 8 February 2016 / Published online: 11 April 2016

Abstract The origin of groundwater in the Sfax aquifer system was studied using environmental isotopic tracers ($\delta^{18}O$, $\delta^{2}H$, and ^{3}H). In total, 164 water samples were analyzed for stable isotopes: 73 collected from the Sfax shallow aquifer, 63 from the Sfax middle aquifer, and 28 from the Sfax deep aquifer. Recent recharge of the groundwater in the Sfax aquifer was identified using tritium concentrations in 82 groundwater samples from different depths. The isotopic ratios of the shallow aquifer range from −5.55 to −1.59 ‰ for $\delta^{18}O$ and from −38.38 to −14.19 ‰ for $\delta^{2}H$, and the isotopic ratios in the middle aquifer range from −6.86 to −2.97 ‰ for $\delta^{18}O$ and from −44.18 to −22.38 ‰ for $\delta^{2}H$. The deep aquifer exhibited markedly lower isotopic values, ranging from −6.70 to −5.70 ‰ for $\delta^{18}O$ and from −42.40 to −38.89 ‰ for $\delta^{2}H$. The mixing proportions inferred from stable isotopic mass balance calculations suggest that the deep aquifer contributes significantly to the middle aquifer through geologic structures and may reach 100 % in the Menzel Chaker region. The isotopic mass balance model also indicates that the middle groundwater aquifer may contribute up to 100 % of the shallow Plio-Quaternary aquifer, particularly in the western and northeastern parts of the study area, between Bir Ali ben Khalifa and Djebeniana. The tritium data support the existence of recent recharge. The tritium and stable isotope data clearly indicate the presence of mixing processes, especially in the northwestern and coastal portions of the study area. A conceptual model is established, explaining the pressure differences that generate vertical leakage, which is a reasonable mechanism for flow between the aquifers.

Keywords Isotopes · Aquifer · Leakage · Recharge · Balance · Sfax

✉ Rahma Ayadi
ayadirahma2285@yahoo.fr

Kamel Zouari
kamel.zouari@enis.rnu.tn

Hakim Saibi
saibi-hakim@mine.kyushu-u.ac.jp

Rim Trabelsi
trabelsi.rim01@gmail.com

Hafedh Khanfir
khanfirafedh@yahoo.fr

Ryuichi Itoi
itoi@mine.kyushu-u.ac.jp

[1] Laboratory of Radio-Analysis and Environment, National School of Engineers of Sfax, Sfax University, BP 1173, 3038 Sfax, Tunisia

[2] Department of Earth Resources Engineering, Faculty of Engineering, Kyushu University, Fukuoka, Japan

[3] Water Resources Division of Sfax, Agriculture Ministry, Sfax, Tunisia

Introduction

Stable isotopes in water have long been used as groundwater tracers (Clark and Fritz 1997) to identify possible recharge areas and mixing within aquifer systems. The identification of recharge sources in semi-arid areas provides insights into recharge processes that are required to develop sustainable water resource management plans within the context of climate variability (Scanlon et al. 2006). Stable and radiogenic isotopes combined with groundwater chemistry can provide helpful tracers for identifying the recharge sources of a groundwater system on both local and regional scales (Edmunds and Tyler

2002). The study of isotopes is an important complementary tool in the evaluation of hydrogeological and hydrochemical processes that affect water masses, such as evaporation and mixing in any groundwater system (Tijani et al. 1996). In this way, isotopic tracers have been used to highlight the origins of water and residence times (Geyh 2000). In Tunisia, particularly in the south of the country, groundwater is the main water resource and is used mainly by agricultural and domestic sectors. The Sfax region, located on the east coast of the country, has a groundwater aquifer system featuring a deep confined aquifer, a middle aquifer and shallow aquifers that are delimited by their respective catchment areas. Recently, water management authorities have been facing problems of declining water quality and increasing water requirements due to a rapidly increasing population and the expansion of agricultural activity. The arid climate coupled with intensive exploitation of groundwater resources is leading to water resource deficits and groundwater quality degradation (Bouchaou et al. 2008; Yangui et al. 2010). The groundwater of the shallow aquifer is over-exploited, with approximately 54.45 Mm^3 of water pumped from this aquifer in 2014, corresponding to a deficit of 21.32 Mm^3 and resulting in seawater intrusion. Most of the water needs in the Sfax basin are supplied by the Miocene deep aquifer, from which approximately 10 Mm^3 of water has been pumped annually from this aquifer between 1978 and 1986. Between 1987 and 2000, the annual amount of extracted water has increased to 26 Mm^3. The exploitation of the deep aquifer reached 112.55 % in 2014. Previous hydrogeological studies of this region (El Batti and Andrieux 1977; Beni Akhy 1994; Maliki 2000; Fedrigoni et al. 2001; Trabelsi et al. 2005) have shown that the Sfax plain contains two main aquifers: a shallow aquifer (Plio-Quaternary) overlying a deep aquifer (Miocene). However, recent studies (Gassara and Ben Marzouk 2009; Hchaichi 2008; Hchaichi et al. 2013) have proved the existence of a middle aquifer in the detrital Mio–Pliocene deposits. The renewable water resources of this middle aquifer were estimated to be 11.3 Mm^3 using the Darcy equation ($Q = L \times T \times i$) (T = transmissivity of 1.23 $\times$ 10^{-3} m^2/s; L = length of the groundwater flow front; i = hydraulic gradient). The Sfax aquifer system constitutes the main water resource in southeastern Tunisia. Intensive exploitation of the aquifer in recent years, due to the continuous population and economic growth in Sfax region, has induced declining water levels and progressive degradation of groundwater quality due to salinization. To implement efficient management of these groundwater resources under heavy anthropogenic stress, quantitative information on the dynamics, origin and regional mixing patterns of the groundwater in the Sfax aquifer are needed. The mixing of waters via upward leakage between deep and shallow aquifers (Maliki et al. 2000) has been confirmed by several previous isotopic studies, and the rate of leakage has been computed. However, for the first time, this paper computes the rates between the deep, shallow and recently identified exploited middle aquifer. The previous quantifications will be updated with respect to the addition of the middle aquifer.

In the present study, the Mio-Plio-Quaternary aquifer system of the Sfax basin was the subject of an isotopic study, which uses a set of stable isotope tracers ($\delta^{18}O$, $\delta^{2}H$) and tritium isotope (^{3}H) to identify the origins of the groundwaters in the Sfax basin. The objectives were to (1) identify the origin of groundwaters of the Sfax aquifer system, (2) estimate the mixing proportions between different aquifers using stable isotopes and (3) verify the occurrence of recent recharge using tritium isotopes in terms of recent versus old waters.

Study area

The Sfax region, located on the eastern coast of Tunisia, is the second largest urban area after Tunis (1.2 million inhabitants). The Sfax basin is bordered to the east by the Mediterranean Sea, the N–S axis (J. Gouleb 736 m, J. Zebbouz 541 m, J. Boudinar 716 m, J. Goubrar 622 m, J. Krechem el Artsouma 655 m) to the west, the J. Korj, J. Bou Thadi, and J. Chorbane to the north and Skhira in the south (Fig. 1). The present study area is characterized by semi-arid climatic conditions with an average annual precipitation of 239 mm (I.N.M. Sfax 2011) and an evapotranspiration of approximately 1829 mm/year in 2011 (I.N.M. Sfax 2011).

Geology and hydrogeology

The geology of the area was described by Castany (1953), Burollet (1956) and Zebidi (1989). The Sahel in the Sfax area is characterized by a repetitive topography of small accented hills, separated by wide basins occupied by sabkhas. The geology of the study area is dominated by outcrops of Mio-Pliocene and Quaternary deposits. Most of the outcrops are affected by the major tectonic phases that have occurred in the region (Ben Akacha 2001). The study area contains long-wavelength anticlines with relief of less than 200 m (Belgacem et al. 2010). The lithology includes the Souar Formation, considered to be of Eocene age and composed of marine sediments (Bouaziz 1994). The Oligocene sediments feature a lower marine unit and an upper continental sandy unit. The Miocene deposits are thick and feature alternating units of clay, sand and sandstone. These deposits are divided into three units (Tayech 1984): the Ain Ghrab Formation (Burdigalian), consisting primarily of

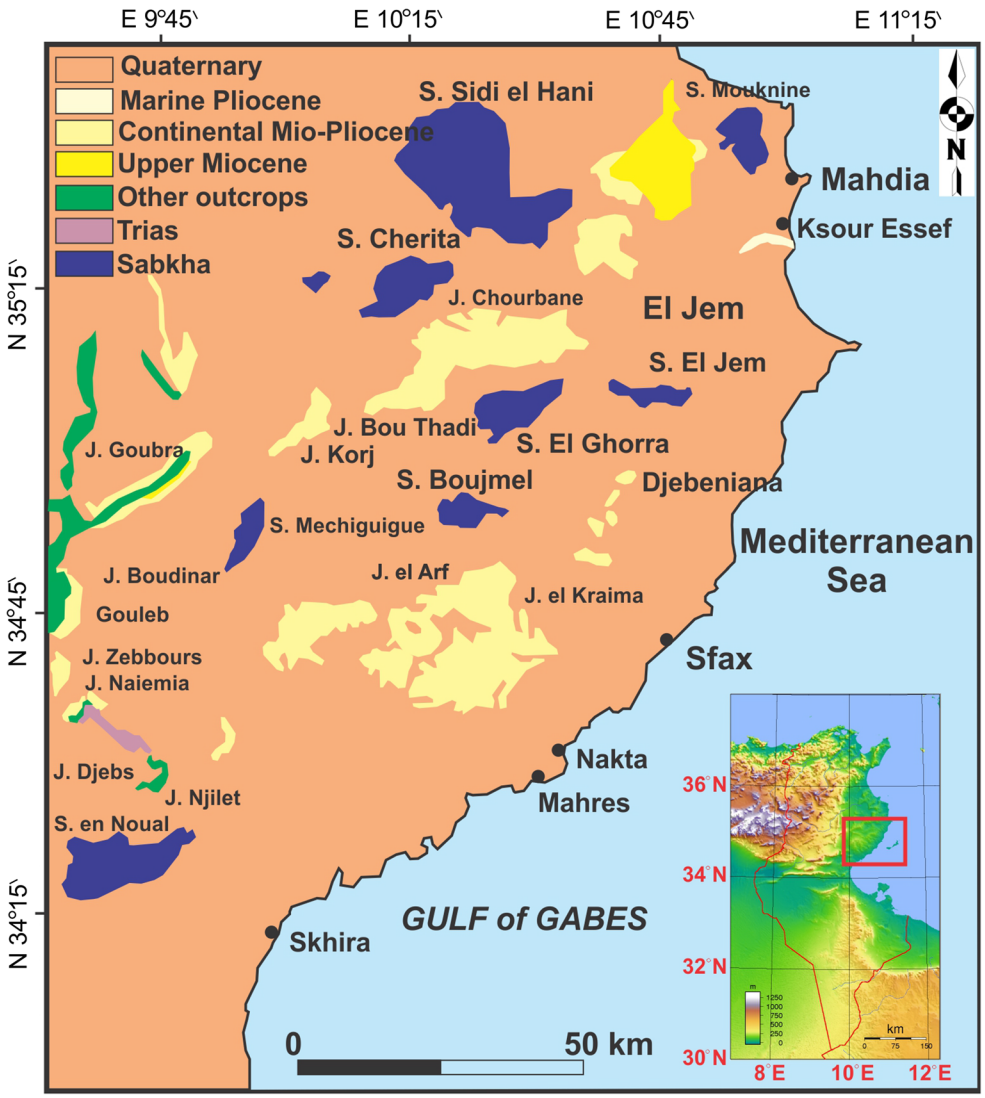

Fig. 1 Location and geological map of the study area (from the geological map of Tunisia at 1/500,000)

limestone interbedded with gypsum in the lower part; the Oum Douil Formation (Langian to Tortonian), consisting of a variable proportion of silt and clay; and the Segui Formation (Messinian), consisting of alternating continental sand, silt and clay. Pliocene marl deposits discordantly overlie the older formations. The Pleistocene is divided into two units: a lower one, characterized by calcareous sand, and an upper one, composed of silt and gypsum. The Holocene deposits are characterized by granular materials of various origins overlying clayey formations. The Upper Miocene, Pliocene and Quaternary sand and silty clay deposits constitute the reservoir of the region's shallow aquifer (Fig. 2). These deposits represent several productive layers separated by semi-permeable layers.

As shown in the hydrogeological NNW–SSE cross section, three aquifers are present in the Sfax basin (Fig. 3).

Shallow aquifer

The shallow aquifer is a phreatic superficial unit located in the Quaternary and Mio–Pliocene deposits, comprising sand and silty clay layers that are separated by sandy-clays (Hajjem 1980; Maliki 2000). The aquifer's thickness varies from 8 to 60 m, with an average of 30 m. The substratum of the reservoir is composed of a clayey–sandy unit of continental origin. It is characterized by alternations of unrefined natural sand and conglomerates, with beds of red sandy marls and clays. Generally, these water-bearing formations have an alluvial nature and are characterized by a lenticular geometry with limited horizontal area and an irregular vertical continuity. Based on pumping tests, the transmissivity was estimated to 1.5×10^{-3} m^2/s (Maliki 2000; Rozanski et al. 1993). The major groundwater flow direction in this aquifer is from NW to SE (Takrouni et al.

Fig. 2 Hydrogeology of the Sfax aquifer system

CHRONOSTRATIGRAPHY		FORMATION		LITHOLOGY	HYDROSTRATIGRAPHICAL FORMATION
Quaternary	Actual Holocene Pleistocene			Actual alluvium silty sands limestone with gypsum	
Mio-Pliocene	Placenzian	Segui		Alternating white and yellow sands with green and brown clays	Aquifer
	Zanclean				
	Messinian				
Miocene	Tortonian	Souaf	Oum Douil	Gray clay with gypsum and silts continental facies	Aquitard
		Beglia		Alternating yellow fine sands and green-brown clays	Aquifer
	Serravallian			Gray clays / marine facies	Aquitard
	Langhian	Ain Ghrab		Sandy limestone/marine facies	Aquifer
Oligocene	Upper Oligocene	Fortuna		Sandy clay sediments	Aquitard
	Lower Oligocene				
Eocene	Upper Eocene	Souar		Clay or marly sediments	

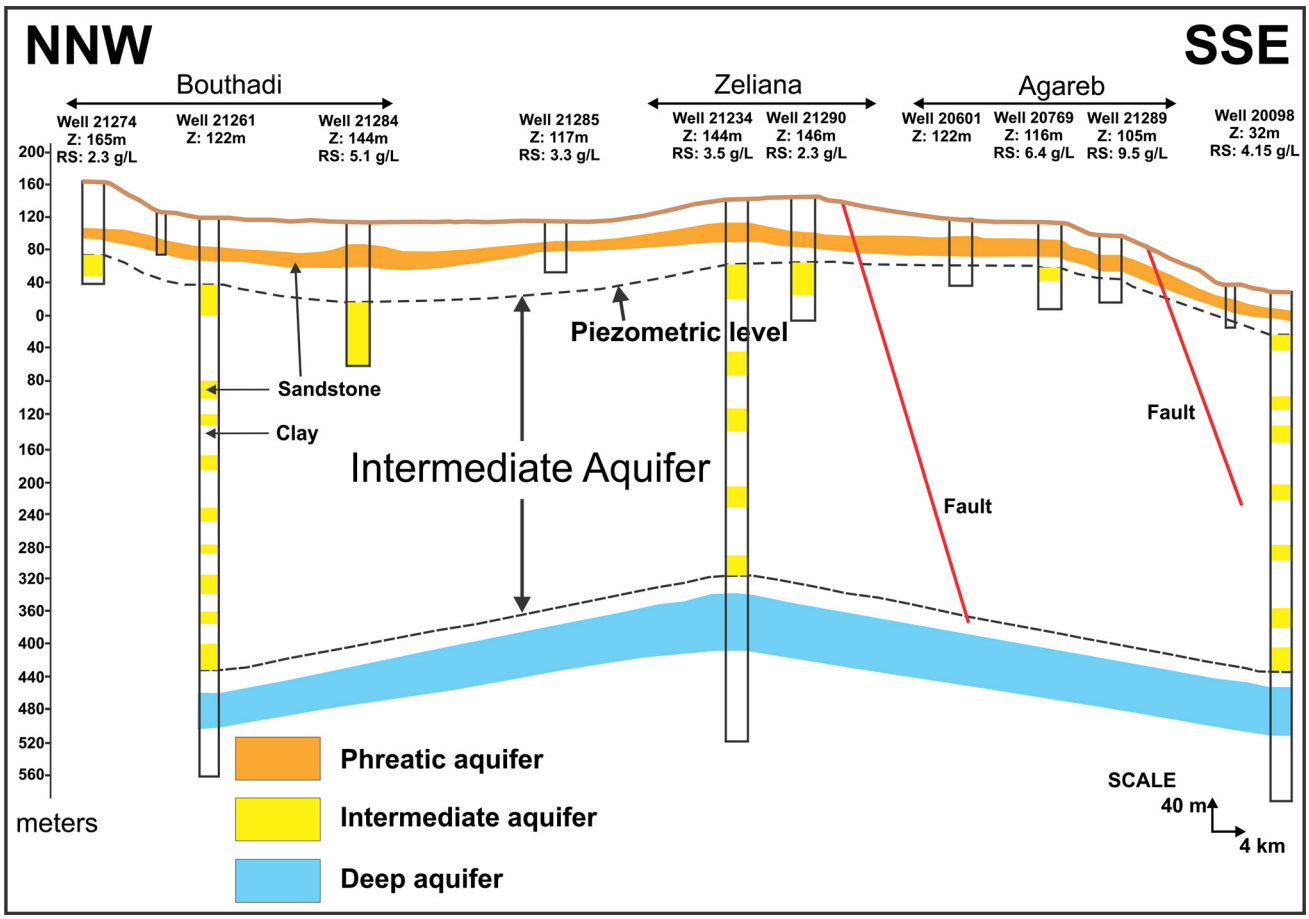

Fig. 3 Hydrogeological cross-section of the Sfax aquifer system (Hchaichi et al. 2013)

2003). The aquifer is recharged mainly by direct infiltration of rainwater. The rapid infiltration is favored by the permeable layers composed of sand and sandy-clay, which are characterized by permeability values ranging from 4×10^{-6} to 68×10^{-4} m/s (Ben Brahim et al. 2011). The aquifer's highest elevations are located in the north and the

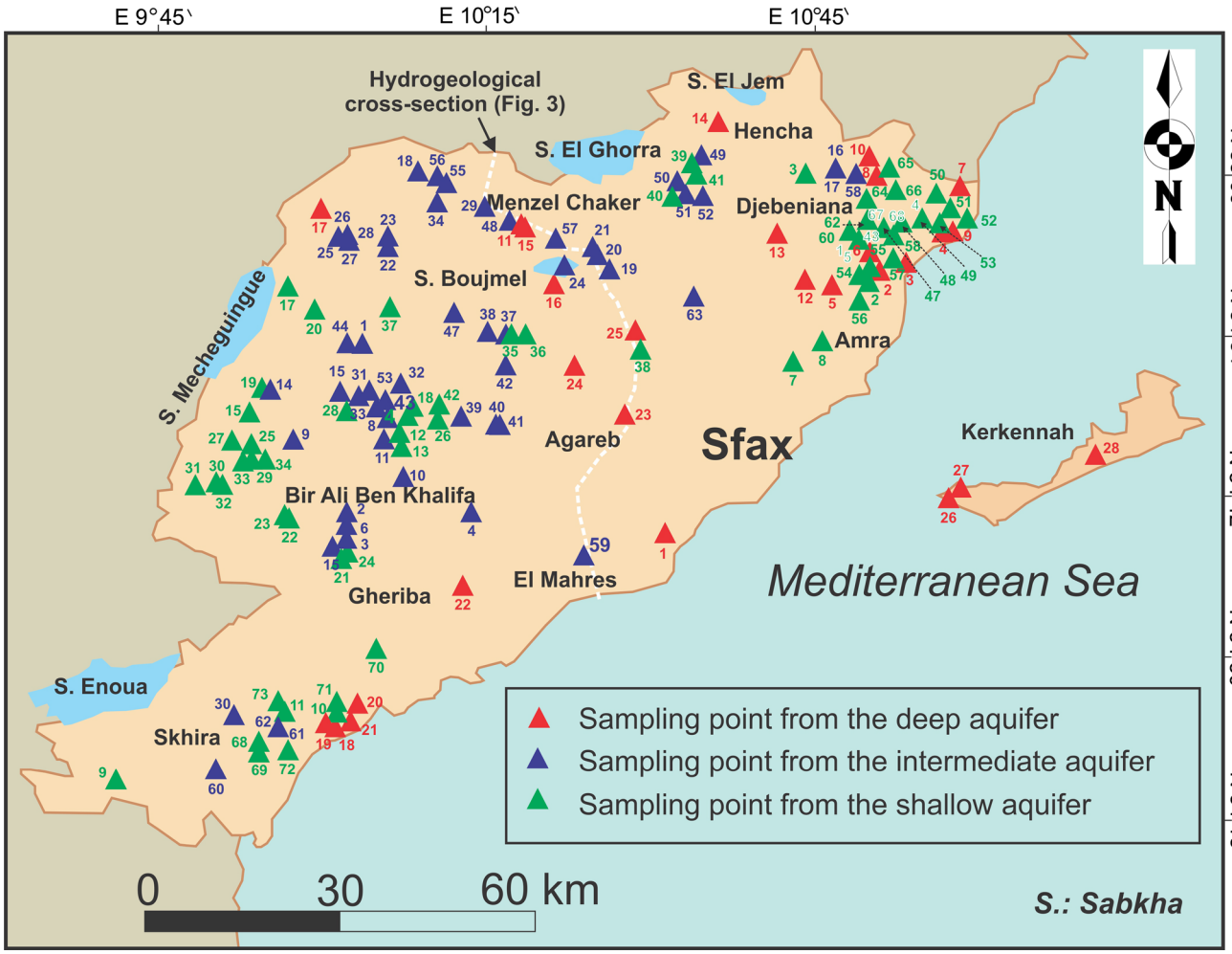

Fig. 4 Location map for isotopic samples

west of the basin, and the Mediterranean shoreline and the sabkhas are its discharge areas. The reserves of the shallow aquifer are limited and have been overexploited by the continuous increase in withdrawal rates, causing salinization (Ben Hamouda et al. 2010) and water-quality degradation, particularly in the coastal areas. These processes threaten the sustainable groundwater resources of the region, leading to difficulties in establishing a suitable management plan of waters especially for irrigation uses.

The middle aquifer

The middle aquifer, situated between the shallow and deep aquifers, has been identified at depths between 70 and 200 m. It consists of 150–300 m of Pliocene and Quaternary sand and sandy-clay deposits. The aquifer's thickness increases from north to south. It constitutes a multilayered aquifer differentiated into several units of detrital sediments separated by clay-rich strata, producing heterogeneity in this aquifer. Several thin, relatively permeable layers may be important in controlling the hydraulic continuity. Transmissivities measured from pumping tests are in the range of 1×10^{-4} to 4.32×10^{-3} m^2/s (Hchaichi 2008; Hchaichi et al. 2013). The water resources of the middle aquifer were estimated to be 11.3 Mm^3/year (C.R.D.A. Sfax. 2012).

Miocene deep aquifer

The Miocene deposits form the deepest aquifer. This aquifer is the principal aquifer of the region. It is hosted in sand and sandstones interbedded with clay. Its thickness varies, and the maximum thickness is observed in the central part of the basin. The thickness decreases towards the Skhira region and is thinnest in the Kerkennah Island region (Trabelsi et al. 2006). This aquifer is located at depths between 200 and 700 m, its average thickness is 250 m, and it covers an area of approximately 15,000 km^2. The deep aquifer is characterized by high transmissivities,

ranging from 0.123×10^{-3} to 130×10^{-3} m^2/s with an average value of 23.32×10^{-3} m^2/s (Trabelsi et al. 2006). The highest transmissivity values, generally approximately 90×10^{-3} m^2/s, are observed in the northern part of the study area, and the lowest values are observed along the coast and in the southern part, where the aquifer is intensively exploited. The deep aquifer is an important water source in the study area because of its relatively significant thickness and its higher water quality relative to the water quality of the overlying aquifers. The groundwater flow directions of this aquifer are generally from the northeast to the southwest, i.e., from the heights of the north–south axis toward the Mediterranean Sea (Skhira region) (Takrouni et al. 2003; Hchaichi et al. 2013). Despite the increasing exploitation coupled with the absence of recent recharge, the piezometric monitoring from 1987 to 2011 showed only an average annual decrease of 0.3 m, revealing the significant reserves of this aquifer (Hchaichi et al. 2013). This aquifer is artesian along the coast and confined in the center of the basin. The extracted water volumes have been raised from 18 Mm^3 in 1988 to 28.7 Mm^3 in 2014 (C.R.D.A. 2015). The aquifer is exploited for various purposes, including agricultural (24 %), industrial (31 %) and domestic uses (45 %) (C.R.D.A. 2015). An analysis of tritium, a radioactive isotope of hydrogen, revealed the absence of actual recharge in the aquifer, indicating a paleoclimatic effect. The deep aquifer was recharged under colder climatic conditions than at present. This paleoclimatic origin is supported by the dating data of carbon 14, which suggests ages between 14,000 and 38,000 years (Maliki et al. 2000).

Materials and methods

For this study, a total of 164 water samples were collected from wells and boreholes with depths ranging from 14 to 200 m (Fig. 4) in the basin of Sfax during sampling campaigns in 2012, 2013 and 2014. Of these groundwater samples, 73 samples were from the shallow aquifer, 63 were from the middle aquifer and 28 were from the deep aquifer. Stable isotope values ($\delta^{18}O$ and $\delta^{2}H$) were measured for all samples. Additionally, 82 samples were selected for tritium analysis.

The stable isotope analyses were performed in the Laboratory of Radio Analysis and Environment (LRAE) at the National Engineering School of Sfax (Tunisia). The stable isotopes analyses ($\delta^{18}O$ and $\delta^{2}H$) were measured using the Laser Absorption Spectrometer LGR DLT 100 (Lis et al. 2008). The $\delta^{18}O$ and $\delta^{2}H$ results are reported in the usual δ notation relative to the Vienna Mean Oceanic Water (V-SMOW) standard, where $\delta = [(R/R_{V\text{-}SMOW}) - 1]/1000$; R represents either the $^{18}O/^{16}O$ or the $^{2}H/^{1}H$ ratio of the sample, and $R_{V\text{-}SMOW}$ is the $^{18}O/^{16}O$ or $^{2}H/^{1}H$ ratio of the V-SMOW standard (Coplen 1996).

The tritium analyses were performed in the LRAE by electrolytic enrichment and liquid scintillation spectrometry (Taylor 1976). The tritium concentrations are reported in Tritium Units (TU), in which one TU equals the isotope ratio $^{3}H/^{1}H = 10^{-18}$.

The precisions of isotope measurements were ±0.1 and ±1 ‰ for $\delta^{18}O$ and for $\delta^{2}H$, respectively, and ±0.3 TU for ^{3}H.

Results and discussion

Stable isotope composition of groundwaters

The stable isotopes ^{18}O and ^{2}H can be used to distinguish between waters from different sources. Hence, they can improve the knowledge of groundwater balance between lakes or reservoirs and an aquifer (Gay 2004; Gonfiantini 1986). The $\delta^{18}O$ and $\delta^{2}H$ values of the shallow aquifer groundwaters range from −1.59 to −5.55 ‰ and from −14.19 to −38.38 ‰, respectively. Those of the middle aquifer samples range from −2.97 to -6.86 ‰ and from −22.38 to -44.18 ‰, respectively. The stable isotope values in the deep aquifer are generally homogeneous. The oxygen and hydrogen isotopic values are lower in the deep aquifer than the values measured in the shallow and middle aquifers, with $\delta^{18}O$ values between −5.70 and −6.70 ‰ and $\delta^{2}H$ values between −38.89 and −42.40 ‰.

The $\delta^{18}O$ and $\delta^{2}H$ values of the groundwater samples are presented in Tables 1, 2 and 3 and are plotted on a $\delta^{18}O/\delta^{2}H$ diagram (Fig. 5), which shows the position of the groundwater samples relative to the Global Meteoric Water Line (GMWL) ($\delta^{2}H = 8 \times \delta^{18}O + 10$; Craig 1961) and the Regional Meteoric Water Line (RMWL) of Sfax ($\delta^{2}H = 8 \times \delta^{18}O + 13.5$; Maliki et al. 2000).

The $\delta^{18}O/\delta^{2}H$ diagram (Fig. 5) shows that most of the groundwater in the Sfax basin plots below the meteoric water lines, except for several points that plot between the GMWL and the RMWL.

Shallow aquifer

According to the position of samples relative to the meteoric water lines in Fig. 5, the Plio-Quaternary aquifer can be divided into three different groups, indicating separate flow paths and recharge areas: the majority of the Sfax shallow groundwater samples are young strongly evaporated groundwater, characterized by $\delta^{2}H$ and $\delta^{18}O$ enrichment with an average values of −4.57 ‰ for $\delta^{18}O$ and −30.62 ‰ for $\delta^{2}H$ (Fig. 5). The sampled groundwater plot near the evaporative enrichment line ($\delta^{2}H = 4.5 \times$

Table 1 Stable isotope values and tritium measurements from the shallow aquifer system

Sample no.	Aquifer	Depth (m)	^{2}H (‰ vs. SMOW)	^{18}O (‰ vs. SMOW)	^{3}H (TU)
1	Shallow	30	−32.43	−4.63	NM
2	Shallow	41	−28.51	−4.07	NM
3	Shallow	14	−22.85	−3.36	NM
4	Shallow	37	−30.08	−4.48	NM
5	Shallow	40	−24.81	−4.10	NM
6	Shallow	30	−31.27	−4.30	NM
7	Shallow		−25.93	−4.07	NM
8	Shallow		−28.05	−4.71	NM
9	Shallow		−33.52	−5.56	NM
10	Shallow		−14.20	−1.60	NM
11	Shallow	30	−27.31	−4.41	1.25
12	Shallow	50	−33.26	−5.40	NM
13	Shallow	45	−30.62	−4.88	5.82
14	Shallow	50	−36.05	−5.32	NM
15	Shallow	67	−37.05	−5.09	NM
16	Shallow	48	−36.11	−5.18	NM
17	Shallow	40	−30.97	−4.48	0.47
18	Shallow	30	−34.27	−5.55	NM
19	Shallow	80	−38.38	−5.36	1.42
20	Shallow	20	−27.60	−4.58	2.01
21	Shallow	35	−35.28	−5.08	NM
22	Shallow	45	−36.00	−5.25	NM
23	Shallow	50	−36.55	−5.15	NM
24	Shallow	35	−32.76	−5.47	NM
25	Shallow	60	−33.25	−5.16	1.14
26	Shallow	41	−32.28	−5.47	NM
27	Shallow	70	−32.22	−4.46	1.39
28	Shallow	45	−30.64	−5.24	4.51
29	Shallow	50	−35.17	−4.95	NM
30	Shallow	50	−34.44	−4.99	NM
31	Shallow	29	−35.17	−5.55	NM
32	Shallow	35	−29.26	−3.92	0.82
33	Shallow	16	−29.03	−3.80	0.48
34	Shallow	45	−34.89	−5.04	NM
35	Shallow	50	−25.67	−4.50	1.75
36	Shallow	17	−24.42	−4.41	NM
37	Shallow	45	−33.81	−4.10	0.70
38	Shallow	90	−31.35	−5.61	0.92
39	Shallow	40	−30.76	−4.73	1.02
40	Shallow	26	−28.07	−3.92	5.06
41	Shallow	45	−29.59	−3.69	0.57
42	Shallow	35	−33.87	−4.08	0.00
43	Shallow		−30.69	−3.67	NM
44	Shallow	57	−31.91	−4.13	0.63
45	Shallow	47	−31.35	−4.05	NM
46	Shallow		−29.87	−4.16	NM
47	Shallow	40	−30.05	−4.12	NM
48	Shallow	73	−27.77	−4.08	0.22
49	Shallow	22	−29.34	−4.48	NM
50	Shallow	20	−27.80	−4.16	1.13

Table 1 continued

Sample no.	Aquifer	Depth (m)	^{2}H (‰ vs. SMOW)	^{18}O (‰ vs. SMOW)	^{3}H (TU)
51	Shallow	34	−29.72	−5.03	0.83
52	Shallow	20	−28.59	−4.92	NM
53	Shallow	29	−23.56	−4.00	1.52
54	Shallow	40	−26.48	−3.64	0.32
55	Shallow	35	−29.85	−4.45	NM
56	Shallow	22	−27.09	−4.42	0.29
57	Shallow	35	−30.00	−4.53	NM
58	Shallow	32	−28.30	−4.70	NM
59	Shallow	42	−27.85	−4.21	NM
60	Shallow	56	−28.30	−4.70	NM
61	Shallow	65	−30.30	−3.93	NM
62	Shallow	76	−31.62	−4.91	0.53
63	Shallow	70	−28.12	−3.79	NM
64	Shallow	82	−33.43	−4.97	NM
65	Shallow	97	−38.38	−5.62	0.65
66	Shallow	70	−35.84	−5.29	NM
67	Shallow	42	−30.34	−4.95	1.01
68	Shallow	24	−32.75	−4.98	1.08
69	Shallow	27	−31.90	−4.81	NM
70	Shallow	12	−31.39	−4.76	1.36
71	Shallow	35	−27.53	−3.69	NM
72	Shallow	26	−29.20	−4.67	1.84
73	Shallow	60	−28.60	−4.35	NM

NM not measured

$\delta^{18}O$ −9.7, $R^2 = 0.6$). A slope of 4.5 is indicative of evaporation from an open water body under conditions of low relative humidity in a semi-arid region (Clark and Fritz 1997). The intersection of the evaporative line with the GMWL gives values of -6 and −38 ‰ for the respective $\delta^{18}O$ and $\delta^{2}H$ contents of the recharging precipitation, before evaporation. The oxygen-18 value of the intersection point is depleted than that of the weighted mean precipitation for Sfax ($\delta^{18}O_{WMPS}$) by approximately 1.4 ‰ for oxygen-18. This can be explained either by an elevation effect or by a paleoclimatic effect. We can verify this hypothesis by calculating the Recharge elevation. The calculated groundwater elevation is approximately 1466 m a.s.l., which is much higher that the elevation of the aquifer outcrops. These groundwaters have been recharged at elevations higher than the elevation of the WMPS station (E_{WMPS} = 10 m a.s.l.). These stable isotope results may also result from the mixture of recent groundwater and ancient groundwater that formed under a different climate. The stable isotope compositions of the evaporated groundwater samples likely resulted from the evaporation effect experienced by the return flow of irrigation water. This irrigation water was pumped from the wells of the shallow aquifer, and the long residence time of the waters allowed it to experience evaporation before returning to the aquifer. The long-term practice of irrigation causes the infiltration of water that commonly experiences intense evaporation in the soil and in the irrigation channels (Ben Moussa et al. 2014). The study area's arid climate would contribute to the strong evaporation of water at the surface and during infiltration through the unsaturated zone before reaching the aquifer. This process supports the enriched isotopic compositions of the groundwater samples relative to those of the WMPS. Certain groundwaters samples (nos. 8, 35, 36, 51 and 52) fall on the GMWL. These samples, with relatively low $\delta^{18}O$ values (−5.1 to −4.5 ‰), likely represent recent meteoric water recharging directly from precipitation, implying rapid infiltration of rainwaters. The isotopic compositions of these samples are close to that of the precipitation ($\delta^{18}O = -4.6$ ‰ and $\delta^{2}H = -23.3$ ‰; Maliki et al. 2000). This non-evaporated groundwater may reflect recharge at lower elevations and depths and may suggest young recharge water originating from infiltrated rainwater masses. The third group represents a mixture of old and young groundwater and is represented primarily by samples from the western part of the basin. The isotopic compositions of most of these samples fall below the global meteoric water line ($\delta^{18}O$ values range from −5.7 to

Table 2 Stable isotope values and tritium measurements from the middle aquifer

Sample no.	Aquifer	Depth (m)	^{2}H (‰ vs. SMOW)	^{18}O (‰ vs. SMOW)	^{3}H (TU)
1	Middle	160	−34.52	−4.97	NM
2	Middle	83	−36.59	−5.18	0.65
3	Middle	100	−35.03	−5.07	NM
4	Middle	71	−31.04	−5.34	3.35
5	Middle	96	−32.24	−5.26	0.87
6	Middle	107	−33.87	−4.95	NM
7	Middle		−31.77	−5.55	4.27
8	Middle	75	−34.00	−5.37	NM
9	Middle	104	−37.06	−5.57	0.97
10	Middle	62	−33.51	−5.56	2.28
11	Middle	73	−32.54	−4.84	0.00
12	Middle	85	−32.56	−5.65	0.47
13	Middle	103	−35.97	−5.13	1.3
14	Middle	145	−37.38	−5.19	1.32
15	Middle	118	−38.90	−5.42	0.73
16	Middle	84	−23.50	−3.36	NM
17	Middle	99	−26.65	−4.22	0.86
18	Middle	123	−36.81	−4.83	NM
19	Middle	164	−34.43	−4.49	0.75
20	Middle	180	−28.34	−3.68	1.53
21	Middle	196	−30.45	−4.48	NM
22	Middle	100	−34.49	−4.97	1.21
23	Middle	100	−34.07	−4.45	NM
24	Middle	84	−34.56	−4.28	NM
25	Middle	95	−37.59	−4.73	NM
26	Middle	98	−35.27	−4.48	0.60
27	Middle	67	−35.88	−4.87	NM
28	Middle	88	−34.45	−4.22	NM
29	Middle	160	−37.72	−4.61	NM
30	Middle	97	−34.90	−5.38	1.01
31	Middle	127	−38.34	−5.17	NM
32	Middle	110	−35.26	−5.40	0.47
33	Middle	70	−33.48	−5.32	NM
34	Middle	110	−34.47	−4.84	NM
35	Middle	100	−36.40	−5.47	0.68
36	Middle	136	−38.23	−5.03	1.36
37	Middle	114	−26.07	−4.39	NM
38	Middle	110	−35.93	−4.89	1.04
39	Middle	110	−37.73	−4.96	0.20
40	Middle	133	−35.79	−5.18	0.60
41	Middle	125	−36.38	−5.57	NM
42	Middle	142	−36.86	−5.17	0.67
43	Middle	103	−27.27	−4.77	0.95
44	Middle	160	−30.73	−4.72	0.20
45	Middle		−37.71	−5.04	NM
46	Middle		−37.90	−5.37	NM
47	Middle	80	−22.38	−2.97	0.00
48	Middle	90	−32.59	−3.47	0.26
49	Middle	94	−29.23	−3.91	NM
50	Middle	80	−27.59	−4.02	1.04

Table 2 continued

Sample no.	Aquifer	Depth (m)	^{2}H (‰ vs. SMOW)	^{18}O (‰ vs. SMOW)	^{3}H (TU)
51	Middle	120	−27.56	−3.76	0.50
52	Middle	120	−30.07	−3.95	0.18
53	Middle	107	−34.06	−6.17	0.00
54	Middle	70	−33.24	−6.14	0.00
55	Middle	137	−33.62	−5.28	0.00
56	Middle	124	−44.18	−6.86	1.07
57	Middle	180	−38.12	−6.30	0.12
58	Middle	125	−33.49	−5.37	0.21
59	Middle	115	−37.51	−5.04	NM
60	Middle	63	−32.01	−4.64	0.25
61	Middle	63	−32.32	−5.07	3.22
62	Middle	60	−32.60	−4.90	1.56
63	Middle	247	−40.14	−5.76	NM

NM not measured

Table 3 Stable isotope values and tritium measurements from the deep aquifer (NM = not measured)

Sample no.	Aquifer	Depth (m)	^{2}H (‰ vs. SMOW)	^{18}O (‰ vs. SMOW)	^{3}H (TU)
1	Deep	573	−41.71	−6.57	NM
2	Deep	570	−39.55	−5.74	0.95
3	Deep	518	−40.49	−5.91	NM
4	Deep	500	−41.68	−5.70	NM
5	Deep	520	−38.89	−5.85	NM
6	Deep	509	−40.90	−6.06	NM
7	Deep	510	−40.47	−6.24	NM
8	Deep	473	−39.99	−6.28	0.86
9	Deep	506	−41.42	−6.14	0.83
10	Deep	452	−40.24	−6.39	0.85
11	Deep	670	−41.20	−6.13	0.05
12	Deep	525	−40.5	−6.30	0.00
13	Deep		−39.14	−5.84	NM
14	Deep	680	−40.35	−6.60	NM
15	Deep	670	−40.59	−6.25	0.20
16	Deep	702	−40.52	−6.17	NM
17	Deep	450	−42.16	−5.93	1.07
18	Deep	263	−42.14	−6.12	NM
19	Deep	240	−42.20	−5.80	NM
20	Deep	276	−42.10	−6.40	0.28
21	Deep	246	−39.80	−6.40	NM
22	Deep	525	−40.60	−6.20	0.00
23	Deep	650	−42.30	−6.10	0.32
24	Deep	523	−40.70	−6.00	NM
25	Deep	332	−40.95	−5.99	0.94
26	Deep		−42.40	−6.50	NM
27	Deep	500	−41.90	−6.70	NM
28	Deep	450	−42.00	−6.01	NM

NM not measured

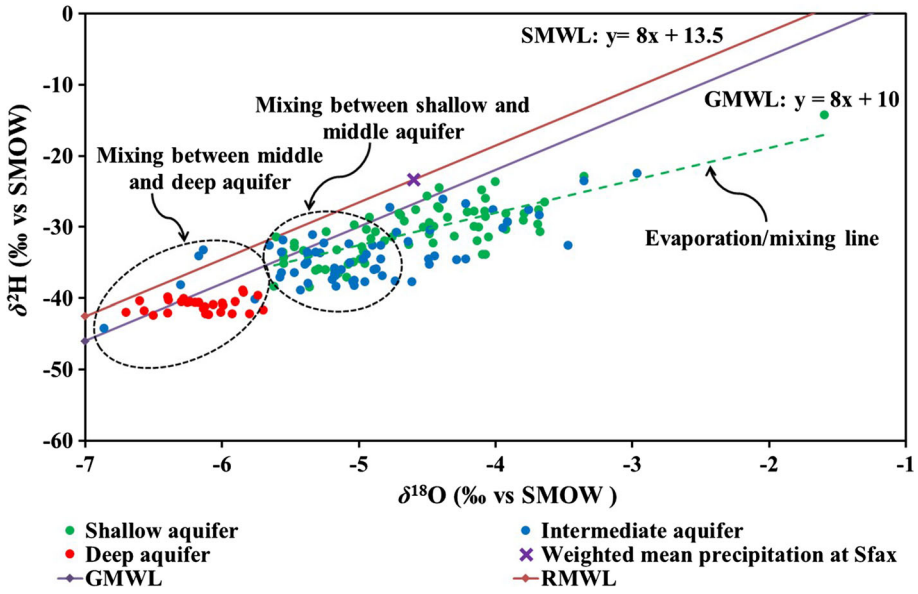

Fig. 5 The δ^2H vs. $\delta^{18}O$ diagram for the groundwater samples from the Sfax basin

−5.1 ‰), likely reflecting upward leakage from the deeper levels into the shallowest aquifer. The leakage in this study is vertical. Hydraulic head differences between the aquifers and overexploitation appear to be the main drivers of upward leakage in the Sfax region. The amount and direction of leakage is governed in each case by the difference in piezometric head that exists across a semipervious formation (Bear 1972). Previous observations made in Sfax basin (Maliki 2000; Takrouni et al. 2003) confirm the contributions of the deep groundwater to the shallow aquifers via upward leakage, which varies from zero to 74 % (Maliki 2000). This mixing process appears to be controlled by tectonic features. This situation suggests a possible communication between the shallow aquifer and the deeper formations of the middle aquifer, which is controlled locally by the semi-permeable layers composed of sands and clayey sands. This observation indicates that the middle aquifer contributes to the recharge of the shallow groundwater, especially in the region of Bir Ali Ben Khalifa in the western part of the Sfax basin.

Middle aquifer

The $\delta^{18}O/\delta^2H$ diagram (Fig. 5) shows that the most of groundwater samples form a group of points that plots below the meteoric water lines and has a regression line of $\delta^2H = 3.75 \times \delta^{18}O - 15.5$, indicating that the water has experienced evaporation. The long-term practice of irrigation causes the infiltration of water that has evaporated in the soil and in the irrigation channels (Ben Moussa et al. 2014). These groundwaters are characterized by relatively high $\delta^{18}O$ and δ^2H values ($\delta^{18}O$ values from −5.6 to −3.4 ‰), which may highlighting the influence of the return flow of irrigation water from the shallow aquifer in the recharge of the middle aquifer. In fact, slower infiltration or seepage of the surface water through stagnant parts of sabkhas, salt depressions on the surface (e.g., sabkha Mechiguigue, sabkha Boujmel and sabkha En Noual), and/or low-permeability layers in the unsaturated zone of the middle aquifer (clayey/evaporitic layers) favors the occurrence of the evaporation effect, leading to an enriched groundwater compositions. The intersection of the evaporation line and the GMWL, at the $\delta^{18}O$ and δ^2H contents of approximately −5.9 and −39 ‰, respectively, is indicative of recharge with water that has not been subjected to extensive evaporation. Because sample nos. 4, 5, 7, 10, and 43 plot above the GMWL, they may represent young groundwaters. The similarity in isotopic composition between these groundwater samples and local precipitation supports a mechanism of rapid infiltration of runoff water before significant evaporation at the soil surface can take place. The isotopic composition of this group of groundwaters ($\delta^{18}O$ values of −5.6 to −4.8 ‰) is close to that of precipitation ($\delta^{18}O = -4.6$ and $\delta^2H = -23.3$ ‰), confirming the relationship of these groundwaters to recent rainwater infiltration. Several other points (nos. 53, 54, 56, 57, and 63) exhibit clearly lower $\delta^{18}O$ and δ^2H values ($\delta^{18}O$ values of −6.86 to −5.76 ‰). This group may represent mixing between old and young water, possibly via upward leakage from the deep aquifer to the middle aquifer, which may explain the depleted isotope compositions of the middle groundwaters. The hydraulic head differences in these aquifers at the northwestern zone due to overexploitation, and most importantly the tectonism (faulting), seem to be the main causes of this per-ascendum flow of the deep groundwater. The mixing process is

mainly through upward leakage of the deep Miocene groundwater replenishing the shallowest Mio-plio quaternary aquifers. The deep Miocene aquifer (200–700 m depths), also called the pressure aquifer, is located above and below impervious formations (Fig. 2) and features a high pressure of approximately 116 atm. This large pressure difference contributes to upward leakage across the semipermeable stratum. Indeed, the elevations of the piezometric surface of the deep aquifer rise above the ground surface toward the coast, generating artesian flow. The wells in these areas flow freely without pumping. The groundwater originating from these mixing and leakage processes are located primarily in the western and northwestern parts of the Sfax basin area. This pattern suggests that the deep aquifer of Sfax contributes to the recharge of the middle aquifer. This process is confirmed by the similar isotopic compositions of the groundwater samples from the two aquifers (Fig. 5). The leakage process appears to be controlled not only by the tectonic features but also by the increasing exploitation of the shallow aquifers, which likely favors upward leakage from the deep aquifer (Maliki et al. 2000).

Deep aquifer

The stable isotope compositions of the deep groundwater samples are homogeneous. The observed variations in the stable isotope values vary between −6.70 and −5.70 ‰ for $\delta^{18}O$ (average −6.15 ‰) and between −42.40 and −38.89 ‰ for $\delta^{2}H$ ‰ (average −40.96 ‰) during the sampling campaigns in December 2013 and January, February and March 2014 (Table 3). The most of points plot primarily below the GMWL, thereby exhibiting significant isotopic depletion. The stable isotope values of the deep groundwater in Sfax are lower than the weighted mean $\delta^{18}O$ and $\delta^{2}H$ values of precipitation ($\delta^{18}O = -4.6$ ‰ and $\delta^{2}H = -23.3$ ‰; Maliki et al. 2000), indicating either recharge at higher elevations or a paleoclimatic effect (recharge under colder climatic conditions than at present). Assuming an ^{18}O gradient with elevation of approximately 0.3 ‰ per 100 m in the precipitation (Blavoux 1978), the calculated recharge elevation for the deep aquifer is between 1366 and 1700 m a.s.l., which is substantially higher than the elevation of the aquifer outcrops (667 m). Therefore, the depleted isotopic composition is likely due to the paleoclimatic effect. This effect may correspond to ancient water that recharged during a period with a cooler climate than that of the present day. Thus, the difference between the isotopic composition of the deep groundwater and that of present precipitation is likely the result of the paleoclimatic effect (Maliki 2000). The hypothesis of paleorecharge is also confirmed by the low ^{14}C concentrations in the deep groundwater, indicating groundwater older than 10,000 years (Maliki et al. 2000). In the plot of $\delta^{2}H/\delta^{18}O$, samples from deep aquifer feature significantly lower $\delta^{18}O$ values, represents mixing with groundwater from the middle aquifer. This process is particularly clear in the recharge areas of Menzel Chaker region observed in samples nos. F56, F57 and F63 and Bir Ali ben Khalifa in samples nos. F53 and F54. This depletion pattern support the mixing with old groundwaters by leakage process. The homogeneity of the stable isotope values and ^{14}C concentrations suggests slow groundwater flow and very weak fluxes from the recharge area in the topographic highs of the north–south axis to the Mediterranean Sea (the Skhira region) (Maliki et al. 2000). The radiocarbon data are very important to characterizing ancient hydrological systems and determining the different rates of mixing between young and old groundwater bodies (Clark and Fritz 1997). The almost 'stagnant' state of this deep coastal aquifer may be related to sea level fluctuations during the recent Quaternary. Starting at approximately 15 ka BP, sea level has increased, reaching a relative plateau at approximately 7 ka BP (Fairbanks 1989). Groundwater flow in the deep aquifer may be primarily controlled by this induced increase in hydraulic head in the coastal discharge zone following the recharge period (Maliki 2000).

Tritium isotope

The tritium content in the groundwater system primarily depends on the original atmospheric concentration at the time of recharge. The radioactive decay that has occurred since infiltration indicates the groundwater age. This requires that the initial tritium value of the precipitation be identified in order to semi-quantitatively interpret the groundwater age from the pattern of tritium values along the groundwater flow path (Ma et al. 2009). In total, 30 shallow wells, 40 boreholes of the middle aquifer and 12 groundwater samples from the deep aquifer were analyzed for tritium content.

In general, water with tritium contents of <1 TU is regarded as having a pre-1952 age, the date that represents the peak in the artificial release of tritium through nuclear (atomic bomb) tests. Such waters are said to have been affected by little or no secondary processes, such as evaporation before infiltration or isotopic exchange with the aquifer materials (Mazor 1991). However, ^{3}H concentrations above 1 TU indicate recent water infiltration, indicating that at least some of the groundwater infiltrated after the early 1950s, therefore featuring ages of <50 years.

The tritium contents of precipitation were measured from rainfall samples collected between 1992 and 2003 at the ENIS meteorological station in Sfax (10 m a.s.l.) (This station is part of the Global Network of Isotopes in

Precipitation, or GNIP). The mean measured value is 5.6 TU (Hchaichi 2008). This tritium value is mentioned in Fig. 7.

For the groundwater samples, the ranges of tritium values in the shallow, middle and deep aquifers are 0–5.82 TU, 0–4.27 TU and 0–1.07 TU, respectively (Fig. 6). These values clearly indicate a local recharge contribution for the groundwaters in the Sfax aquifer system. This contribution is particularly evident in the shallow and middle aquifers and to a lesser degree in the deep aquifer, which features negligible tritium values. These low tritium values are characteristic of ancient recharge, which likely occurred during a cool regime in the past. These observations agree with the results of several studies in southern Tunisia, which were interpreted to indicate that recharge occurred during the late Pleistocene and early Holocene periods (Edmunds et al. 2003; Zouari et al. 2003; Kamel et al. 2008; Kamel 2010). The paleoclimatic origin of the deep aquifer groundwater is also supported by the negligible radiocarbon content, which corresponds to ages of 14,000 to 38,000 years (Maliki 2000).

The relationship between the tritium and stable isotopic values (Fig. 7) confirms that the groundwaters of Sfax have experienced recent recharge, except for the deep aquifer, which contains ancient water with low tritium values (<1 TU) and stable isotope compositions (^{18}O and ^{2}H) that reflect recharge under colder climatic conditions than the present day. The relatively low values seems to be the result of pre-nuclear recharge and/or a mixture between pre-nuclear and contemporaneous recharge.

The high tritium activities (>1 TU) and the groundwater isotopic values that are similar to those of the local precipitation observed in the shallow aquifer indicate recent recharge through the rapid infiltration of rainwater. The highest tritium values are observed in the northeastern part of Sfax basin, i.e., mainly in the northeastern part of Menzel Chaker (sample no. 40), east of Bir Ali Ben Khalifa (sample nos. 13, 19, 20, 27, and 28), Djebeniana (sample nos. 50 and 53) and Skhira (sample nos. 11, 70, and 72). These areas, which feature tritium values larger than 1 TU (Fig. 8), confirm the presence of recent infiltrated water. Several samples in this group (sample nos. 13, 28 and 40) are located in the recharge area (northwestern part) and have high tritium values that are slightly lower than the tritium values measured in the collected Sfax precipitation (5.6 TU) at the ENIS meteorological station. However, certain groundwater samples yielded low or undetectable tritium concentrations, such as sample nos. 17, 33, 41, 42, 48, 54, 56, 62 and 65 (Table 1). The lack of

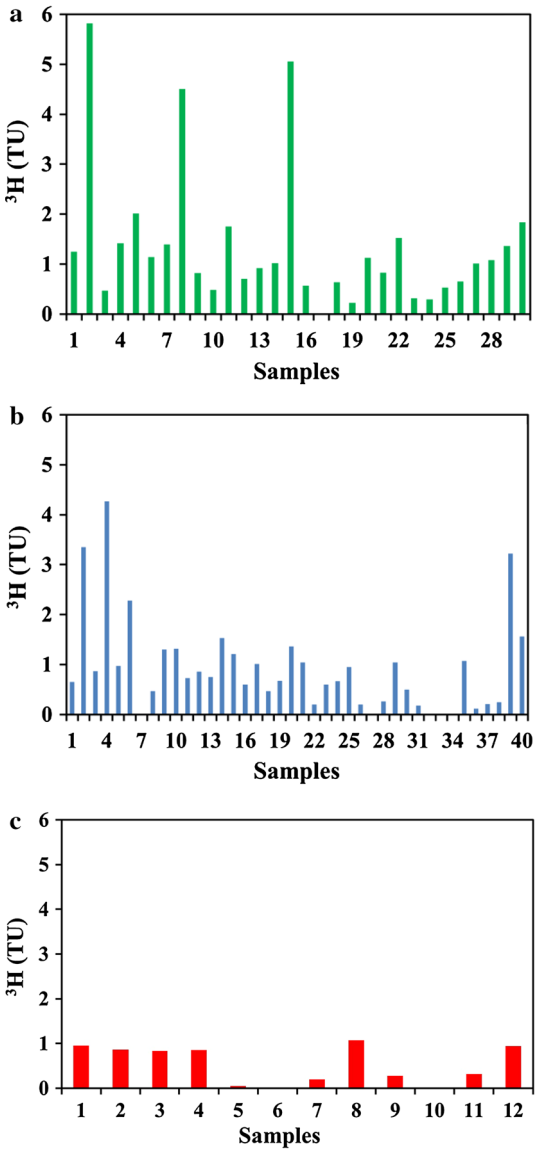

Fig. 6 ^{3}H activities of the groundwater samples from the Sfax basin: **a** the shallow aquifer, **b** the middle aquifer, and **c** the deep aquifer

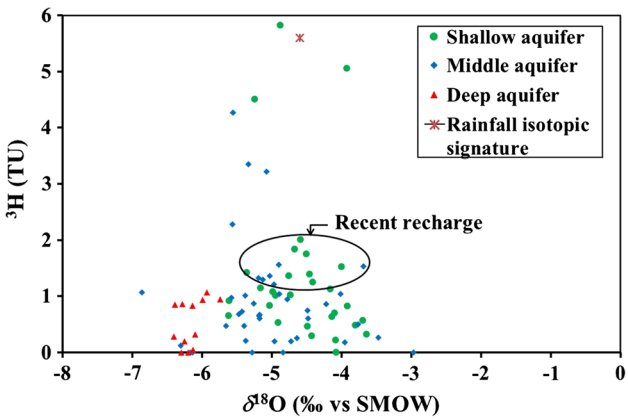

Fig. 7 $\delta^{18}O/^{3}H$ relationship of the groundwater samples in the Sfax basin

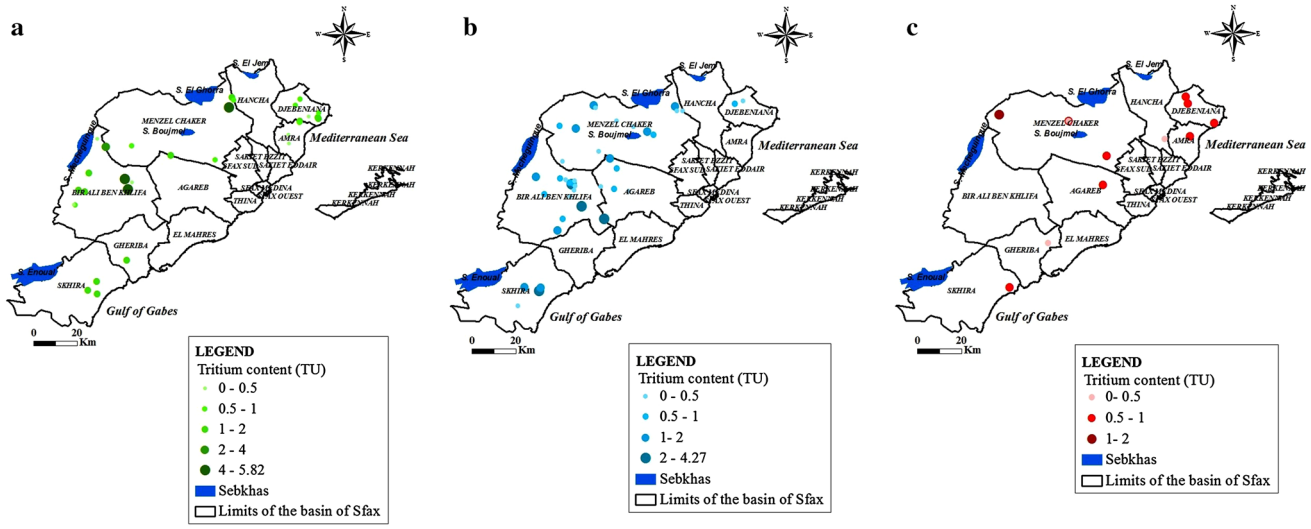

Fig. 8 Tritium distribution map: **a** the shallow aquifer, **b** the middle aquifer, and **c** the deep aquifer

significant tritium in these samples is likely due to mixing processes associated with the migration of groundwater from the middle aquifer to the shallowest aquifer levels. These mixing processes are influenced by the transmissivity of the aquifers' clayey formations, which delay the infiltration of water, thereby increasing the groundwater residence time. Indeed, the presence of tritium values below 1 suggests a mixing process between saline sabkhas groundwater and a source of contamination with a tritium value of 0.83 TU (sample 32). These results also confirm the significance of the atmospheric processes (meteoric water, evaporation, surface wadi water, sabkhas, etc.). Thus, we conclude that the waters from the phreatic aquifer have two principal recharge sources: the middle groundwater aquifer and rainwater. An additional source may be seawater intrusion, particularly in the coastal areas (Takrouni et al. 2003; Trabelsi et al. 2005; Trabelsi 2008), which should be confirmed by combining the current isotope datasets with geochemical approaches.

Several tritium concentrations in the middle aquifer are greater than 1 TU, revealing the occurrence of recent recharge by rainfall infiltration (Fig. 8). These values are primarily observed in samples located in the Bir Ali Ben Khalifa and Menzel Chaker regions, as well as a portion of the Skhira region (sample nos. 30, 61, and 62). The outcrops of the Mio-Pliocene formations are considered to be the infiltration zone, which constitutes the recharge area. The tritium contents measured in sample nos. 4 and 7, which are located in the recharge area (western part), are similar to the weighted mean value of Sfax precipitation (5.6 TU), indicating rapid water infiltration through the wadi of Chaal. In contrast, most of the groundwater samples have lower or undetectable ^{3}H concentrations below than 1 TU, ranging from 0 to 0.9 TU (Table 2), indicating that recent recharge is very limited in the middle aquifer. Mixing with water from the deep aquifer, the significant depth and the low transmissivity of the clayey levels interbedded with sandstones all likely contribute to these low tritium levels, which indicate an old component is present in the middle aquifer. The presence of clay sediments extends contact times, leading to longer groundwater residence times.

Most of the groundwater samples from the deep aquifer have low tritium values between 0 and 0.95 (Table 3); only sample no. 17 produced a tritium value as high as 1.07 TU (Fig. 8). These negligible values confirm that the groundwater from the deep aquifer (200–700 m depth) are old waters. This is consistent with its isotopic signature and therefore with the low carbon content as cited previously. Hence, these data give reasonable idea of the non-tritium content in the samples. The hydrogeological aquifer formations composed of clayey and sandy clays levels interbedded with sandstones contributes to delay the water infiltration in the unsaturated zone and hence to increase the groundwater residence time until reaching the deep aquifer. The age of the groundwater is likely greater than 10,000 years, and the groundwater can be regarded as "fossil" water (Maliki et al. 2000). The measured tritium values, i.e., mostly <1 TU, support the absence of modern recharge.

Isotope balance model

The long residence times, the hydraulic head differences between the Mio-Plio-Quaternary aquifers and the overexploitation appear to be the main drivers of upward leakage in the Sfax basin.

Table 4 Results of the isotopic mass balance calculations

Sample no.	Aquifer	^{2}H isotope balance (%)	^{18}O isotope balance (%)
1	Shallow	86.17	10.40
2	Shallow	49.24	0.00
3	Shallow	0.00	0.00
4	Shallow	64.04	0.00
5	Shallow	14.26	0.00
6	Shallow	75.23	0.00
7	Shallow	24.82	0.00
8	Shallow	44.81	32.40
9	Shallow	96.48	100.00
10	Shallow	0.00	0.00
11	Shallow	37.90	0.00
12	Shallow	94.03	100.00
13	Shallow	69.11	84.40
14	Shallow	100.00	100.00
15	Shallow	100.00	100.00
16	Shallow	100.00	100.00
17	Shallow	72.41	0.00
18	Shallow	100.00	100.00
19	Shallow	100.00	100.00
20	Shallow	40.62	0.00
21	Shallow	100.00	100.00
22	Shallow	100.00	100.00
23	Shallow	100.00	100.00
24	Shallow	89.30	100.00
25	Shallow	93.96	100.00
26	Shallow	84.81	100.00
27	Shallow	84.19	0.00
28	Shallow	69.35	100.00
29	Shallow	100.00	100.00
30	Shallow	100.00	100.00
31	Shallow	100.00	100.00
32	Shallow	56.30	0.00
33	Shallow	54.11	0.00
34	Shallow	100.00	100.00
35	Shallow	22.34	0.00
36	Shallow	10.57	0.00
37	Shallow	99.20	0.00
38	Shallow	76.02	100.00
39	Shallow	70.42	39.49
40	Shallow	45.01	0.00
41	Shallow	59.41	0.00
42	Shallow	99.83	0.00
43	Shallow	69.82	0.00
44	Shallow	81.28	0.00
45	Shallow	76.02	0.00
46	Shallow	62.09	0.00
47	Shallow	63.76	0.00
48	Shallow	42.21	0.00
49	Shallow	57.01	0.00
50	Shallow	42.53	0.00

Table 4 continued

Sample no.	Aquifer	^{2}H isotope balance (%)	^{18}O isotope balance (%)
51	Shallow	60.66	100.00
52	Shallow	49.98	97.96
53	Shallow	2.41	0.00
54	Shallow	30.02	0.00
55	Shallow	61.87	0.00
56	Shallow	35.77	0.00
57	Shallow	63.26	0.00
58	Shallow	47.19	29.22
59	Shallow	42.99	0.00
60	Shallow	47.19	29.22
61	Shallow	66.07	0.00
62	Shallow	78.58	93.63
63	Shallow	45.55	0.00
64	Shallow	95.66	100.00
65	Shallow	100.00	100.00
66	Shallow	100.00	100.00
67	Shallow	66.51	100.00
68	Shallow	89.27	100.00
69	Shallow	81.19	63.92
70	Shallow	76.38	47.22
71	Shallow	39.95	0.00
72	Shallow	55.74	20.09
73	Shallow	50.08	0.00
1	Middle	63.53	23.85
2	Middle	75.26	37.32
3	Middle	66.43	30.23
4	Middle	43.81	47.46
5	Middle	50.60	42.28
6	Middle	59.87	22.28
7	Middle	47.95	61.54
8	Middle	60.61	49.88
9	Middle	77.91	62.90
10	Middle	57.82	62.22
11	Middle	52.34	15.34
12	Middle	52.46	67.86
13	Middle	71.72	34.07
14	Middle	79.72	38.18
15	Middle	88.33	53.20
16	Middle	1.12	0.00
17	Middle	18.96	0.00
18	Middle	76.51	14.63
19	Middle	63.04	0.00
20	Middle	28.52	0.00
21	Middle	40.48	0.00
22	Middle	63.36	23.78
23	Middle	61.01	0.00
24	Middle	63.77	0.00
25	Middle	80.91	8.64
26	Middle	67.80	0.00

Table 4 continued

Sample no.	Aquifer	^{2}H isotope balance (%)	^{18}O isotope balance (%)
27	Middle	71.25	17.51
28	Middle	63.12	0.00
29	Middle	81.64	0.85
30	Middle	65.71	50.24
31	Middle	85.19	36.59
32	Middle	67.74	51.38
33	Middle	57.66	46.32
34	Middle	63.25	15.49
35	Middle	74.18	56.13
36	Middle	84.56	27.88
37	Middle	15.71	0.00
38	Middle	71.53	18.63
39	Middle	81.72	23.06
40	Middle	70.74	37.24
41	Middle	74.05	62.27
42	Middle	76.76	37.07
43	Middle	22.48	11.21
44	Middle	42.08	7.83
45	Middle	81.62	28.70
46	Middle	82.65	49.63
47	Middle	0.00	0.00
48	Middle	52.60	0.00
49	Middle	33.59	0.00
50	Middle	24.27	0.00
51	Middle	24.12	0.00
52	Middle	38.32	0.00
53	Middle	60.94	100.00
54	Middle	56.27	99.19
55	Middle	58.42	43.92
56	Middle	100.00	100.00
57	Middle	83.94	100.00
58	Middle	57.70	49.99
59	Middle	80.44	28.14
60	Middle	49.35	2.65
61	Middle	51.06	30.49
62	Middle	52.67	19.46
63	Middle	95.36	74.84

NC no contribution, values ≤0, represented by 0 %, *MC* maximum contribution, values ≥100 %, represented by 100 %)

Quantification of the mixing proportions in the Sfax basin has been previously performed (Maliki 2000; Maliki et al. 2000; Takrouni et al. 2003). The results showed that the contributions from the deep groundwater to the shallow aquifers in Sfax basin ranges from zero to 74 %. These previous estimates were based on a conceptual model of only two aquifers, the shallow aquifer and the deep aquifer.

This study quantified the contributions from the deep aquifer to the shallow aquifer based on the new data. The equation of the mass balance using $\delta^{18}O$ or $\delta^{2}H$ is formulated as follows:

$$\delta E_{ns} = X\delta E_{np} + (1-X)\delta E_{p} \quad (1)$$

where X represents the contribution (%) of the middle or deep aquifer, and δEns, δEnp and δEp are the ^{18}O or ^{2}H

values of the shallow groundwater, middle groundwater and precipitation, respectively.

Two fluxes should be estimated separately, the first representing the relationship between the deep aquifer and the middle aquifer and the second representing the leakage from the middle aquifer to the shallow aquifer as is highlighted in the $\delta^2H/\delta^{18}O$ diagram.

The mean $\delta^{18}O$ and δ^2H values of −4.93 and −33.89 ‰, respectively, were used for the middle groundwater. For the deep aquifer, the mean $\delta^{18}O$ and δ^2H values were −6.15 and −40.96 ‰, respectively. Finally, the weighted mean values of precipitation ($\delta^{18}O = -4.6$ ‰ and $\delta^2H = -23.3$ ‰; Maliki et al. 2000) correspond to the isotopic composition of rainfall events greater than 5 mm.

The mixing proportions for both scenarios (deep aquifer/middle aquifer and middle aquifer/shallow aquifer) were calculated independently for ^{18}O and ^{2}H, and the results are presented in the Table 4.

Based on Eq. (1) using ^{18}O, the computed contribution of the middle aquifer to the shallow aquifer system ranges from 0 to 100 % (Table 4). The high contribution values are observed primarily in the western part of Sfax and locally in the coastal areas (Djebeniana and Skhira). The contributions of the deep aquifer to the middle aquifer are large, achieving values as high as 100 % in four of the boreholes located in Bir Ali ben Khalifa and Menzel Chaker (in the western and northwestern parts of the Sfax region, respectively). The contribution of the deep aquifer decreases progressively toward the coast, where the recharge is likely dominated by rainwater. The mixing rates seem to be somewhat controlled by depth. However, the thickness of the aquifer decreases toward the coast, which may explain the low leakage rates associated with samples located near and along the coastal areas, e.g. sample nos. 3, 5, 7, 10, 35, 36 and 53. This pattern highlights the recharge of the shallow aquifer from other sources, such as rainwater and marine intrusions, particularly in coastal wells.

Based on the deuterium mass balances, most of the investigated groundwaters presented significant mixing proportions, with mean contribution values of approximately 67 and 60 % for middle aquifer contributions and deep aquifer contributions, respectively. These significant percentages show the importance of leakage between the semi-permeable layers in the recharge of the Sfax aquifer system. For the deep–middle aquifer interaction, the highest mixing proportions are observed in Bir Ali Ben Khalifa and Menzel Chaker. In contrast, the vertical leakage of the deep aquifer is insignificant in the coastal part of the Djebeniana region (sample nos. 16 and 17) and locally in the northern and central parts of the basin (sample nos. 47, 50, and 51), where the contributions are low. The highest calculated values are observed in the western and northwestern parts of the basin, where the contributions reach 100 % for the relationship between the middle-shallow aquifer. These values are generally lower in the coastal part, particularly in the Djebeniana region (sample nos. 3, 5, 10, 24, 53, etc.), and the central part (sample nos. 35 and 36) (Table 4). The low mixing proportions in these wells may be related to the contribution of rainwater infiltration and the possible marine intrusion in the coastal wells due to the shallow well depths and proximity to the coast. These factors contribute to the recharge of the aquifer via direct water infiltration (the permeability values are between 4.10^{-6} and 68×10^{-4} m/s) (Ben Brahim et al. 2011). The recharge of the shallow aquifer is largely controlled by atmospheric exchange (precipitation and evaporation), the middle aquifer and likely seawater intrusion in the coastal northern portion of the basin (Maliki et al. 2000; Fedrigoni et al. 2001; Takrouni et al. 2003).

These findings suggest that in these areas, the aquifer recharge is not derived solely from the mixing process but from the infiltration of precipitation and likely marine intrusion in coastal wells located in the Djebeniana and Skhira regions (Trabelsi et al. 2005). The shallow depths of these wells and their proximity to the coast favors rapid

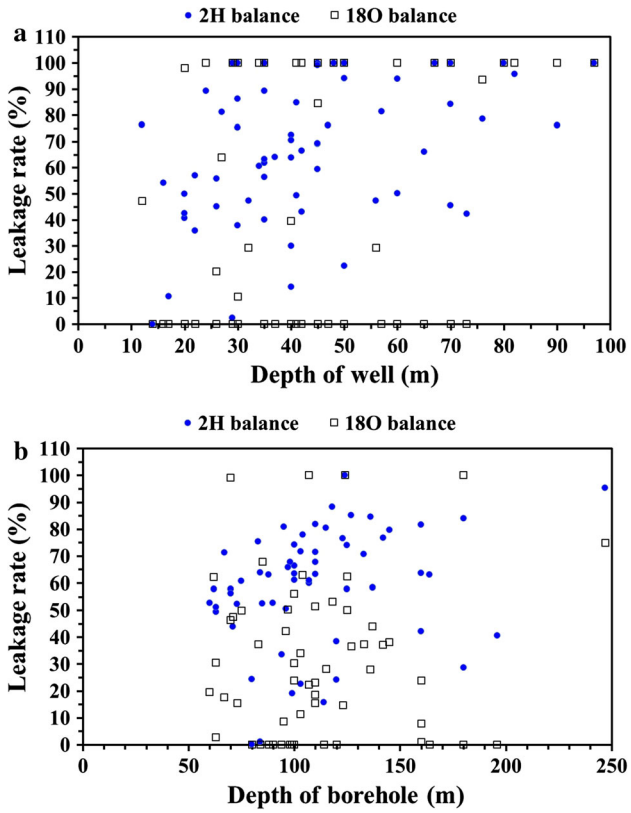

Fig. 9 Diagram of mixing proportion (%) versus sample depth using deuterium and oxygen-18 balance for **a** the contribution of the middle aquifer to the shallow aquifer and **b** the contribution of the deep aquifer to the middle aquifer

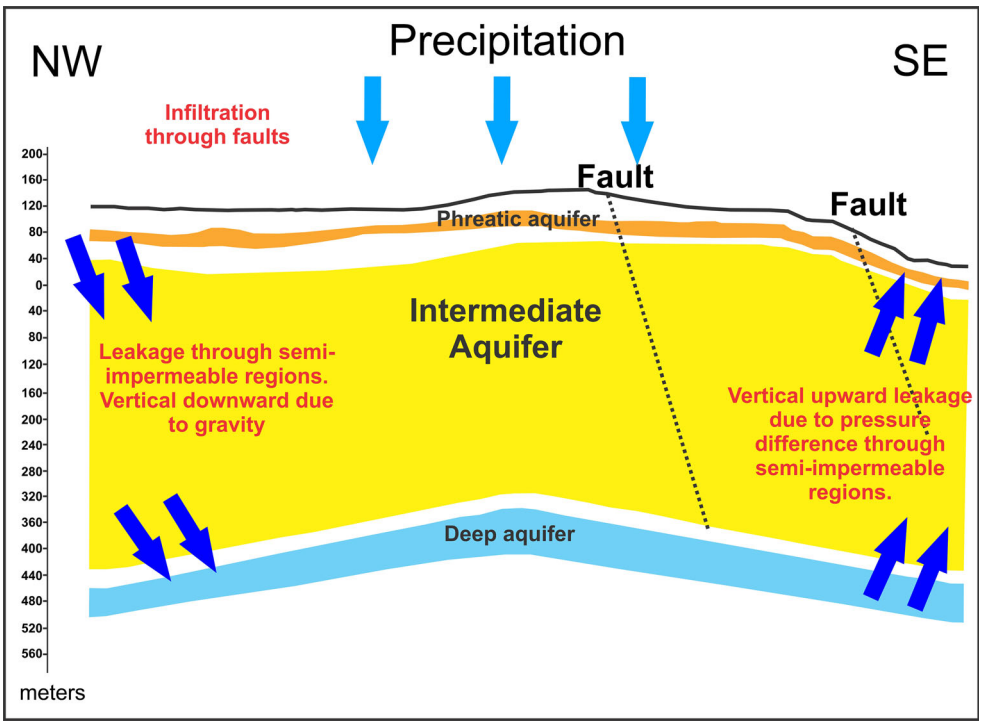

Fig. 10 Conceptual groundwater dynamics model showing the vertical leakage process

recharge via rainwater infiltration and the possible contamination by Mediterranean water masses.

The mixing proportion calculations show several important differences between the ^{18}O and ^{2}H balances (Fig. 9). These differences are related to the fact that the representative groundwater data points are not on a pure mixing line between precipitation and deeper groundwaters. Such differences in the computed values for some samples exist when using ^{18}O and ^{2}H as a δ parameter. The isotope values are controlled not only by a mixing phenomenon but also by other process that should be taken into consideration. They may derive from the more prominent evaporation process (for the stable isotopes), which tends to enrich more ^{18}O than ^{2}H or even dilution. For example, evaporation may affect the water during infiltration, and the contribution of seawater may alter the isotopic values, especially in the shallow coastal areas. Both of these process tend to increase isotopic values. The contribution estimates based on the ^{2}H balance appear to be the most reliable and precise, but they must be considered as minimum values. The results are precise values that do not feature many 0 % contributions. However, the computed results obtained using the ^{18}O balance feature many 0 % values that indicate estimate not possible about the mixing ratios. Therefore, these values must be considered to be minimum values (Maliki et al. 2000).

These results are useful for groundwater evaluation and management in the Sfax basin, especially with the dramatic increase in exploitation and other anthropogenic impacts.

Conclusions

The Sfax aquifer system is among the most important groundwater systems in southern Tunisia. This multilayer aquifer is composed of a deep aquifer in Upper Miocene sands and a shallow aquifer in Mio-Plio-Quaternary sands and sandy clays. The reliable assessment of the system's groundwater resources is important to planning for the demographic and economic development of the region. The stable isotopic compositions of the groundwaters in the Sfax region have been analyzed to provide basic information on their origin and to identify interactions and mixing rates between the deep, middle and shallow aquifers. The stable isotopic values show that the upper Sfax groundwaters are primarily young, evaporated infiltrated precipitation. The isotopic values of these samples are typical for water that has been subject to open surface evaporation in semi-arid regions. However, two other groups of groundwaters were also identified: young groundwater derived from rainwater associated with rapid infiltration and mixed groundwaters with markedly lower ^{18}O and ^{2}H isotopic values, indicating the interaction between the different Sfax aquifer layers. The deep aquifer consists of ancient groundwater with low isotopic values, which are distinguishable from those of the shallow and the middle aquifers. The results of this study confirm the presence of large-scale interactions between the deep, middle and shallow aquifers. The leakage process (Fig. 10) is confirmed by the isotope mass balance

calculations. The mixing proportions inferred from the stable isotope mass balance calculations demonstrate the existence of two types of upward leakage in the Sfax basin: (1) leakage from the deep aquifer to the middle aquifer and (2) leakage from the middle aquifer to the shallow aquifer. These contributions, quantified by isotope mass balance calculations, are highly variable and in places reach 100 %. The increasing exploitation of the shallow aquifers appears to be driving vertical leakage from the deeper levels, which are also heavily exploited at present. The deep aquifer almost appears to be in a 'stagnation state' with slow horizontal circulation. The contribution proportions of the deep aquifer to the middle aquifer are large and may even reach 100 % in the Bir Ali ben Khalifa and Menzel Chaker regions. The contribution of the middle aquifer to the shallow aquifer is observed primarily in Bir Ali ben Khalifa and locally in the Djebeniana and Skhira regions, where it reaches 100 %.

The tritium analyses provide evidence of the presence of modern recharge, but several Mio-Plio-Quaternary groundwater samples show low to undetectable tritium concentrations, likely due to the large depths of the middle aquifer and the migration of groundwaters from deeper levels to shallower aquifer levels. The low transmissivities in the evaporitic deposits (gypsum/anhydrite) may also contribute to decreasing the tritium content by increasing the groundwater residence time.

This assessment should be corroborated through comparison with the results of chemical analyses of the collected samples, especially for the coastal aquifers, which are likely contaminated with seawater. Using chloride concentrations or isotopic mass balance equations, a future analysis could quantify the contribution of seawater to the groundwaters. A study that combines chemical and isotopic approaches will be able to precisely define the mixing endmembers involved in recharging the Sfax aquifers and more precisely quantify their respective contributions.

Acknowledgments The authors would like to thank the technical staff of the Laboratory of Radio-Analyses and Environment at the National Engineering School of Sfax (ENIS) for the chemical and isotopic analyses. Special thanks are also given to the staff members of the Regional Direction of Agriculture and Water Resources of Sfax (South Tunisia) for assistance with the field work.

References

Bear J (1972) Dynamics of fluids in porous media. Dover, New York, p 764

Belgacem A, Kharroubi A, Bouri S, Abida H (2010) Contribution of geostatistical modelling to mapping groundwater level and aquifer geometry, case study of Sfax's deep aquifer. Tunis Middle East J Sci Res 6(3):305–316

Ben Akacha M (2001) Etude géologique de la région d'Agareb-Sfax: évolution géomorphologique néotectonique et paléogéographique. DEA, Fac. Sc., Sfax

Ben Brahim F, Bouri S, Khanfir H (2011) Hydrochemical analysis and evaluation of groundwater quality of a Mio-Plio-Quaternary aquifer system in an arid regions: case of El Hancha, Djebeniana and El Amra regions, Tunisia. Arab J Geosci 6:2089–2102. doi:10.1007/s12517-011-0481-6

Ben Hamouda MF, Tarhouni J, Leduc C, Zouari K (2010) Understanding the origin of salinization of the Plio-Quaternary eastern coastal aquifer of Cap Bon (Tunisia) using geochemical and isotope investigations. J Environ Earth Sci 63:889–901

Ben Moussa A, Mzali H, Zouari K, Hezzi H (2014) Hydrochemical and isotopic assessment of groundwater quality in the Quaternary shallow aquifer, Tazoghrane region, north-eastern Tunisia. J Quat Int 338:51–58

Beni Akhy R (1994) Evolution et modélisation de la nappe phréatique urbaine de Sfax. Mémoire de DEA, Fac. Sc., Tunis

Blavoux B (1978) Etude du cycle de l'eau au moyen de l'oxygène 18 et du deutérium, thèse d'État, université Paris-6, p 316

Bouaziz S (1994) Etude de la tectonique cassante dans la plate-forme et l'Atlas Saharien (Tunisie meridionale): évolution des paléochamps de contraintes et implication géodynamique, Thèse Doctorat. Etat. Sc. Geol, Univ. Tunis II, Tunis

Bouchaou L, Michelot JL, Vengosh A, Hsissou Y, Qurtobi M, Gaye CB, Bullen TD, Zuppi GM (2008) Application of multiple isotopic and geochemical tracers for investigation of recharge, salinization, and residence time of water in the Souss-Massa aquifer, southwest of Morocco. J Hydrol 352:267–287

Burollet (1956) Contribution à l'étude Stratigraphique de la Tunisie Centrale, Annale des mines et de la Géologie 18, Tunisia, p 345

Castany G (1953) Les plissements quaternaires en Tunisie. Comptes Rendus Sommaires Société Géologique de France, Paris, pp 155–157

Clark ID, Fritz P (1997) Environmental isotopes in hydrogeology. CRC Press/Lewis Publishers, Boca Raton

Coplen TB (1996) New guidelines for reporting stable hydrogen, carbon, and oxygen isotope-ratio data. Geochim Cosmochim Acta 60:3359–3360

Craig H (1961) Isotopic variation in meteoric water. Science 133:1702–1703

C.R.D.A (2012) Exploitation de la nappe profonde en 2011. Annuaires d'exploitation des nappes aquifères de Sfax. Commissariat Régionale d'Activité Agricole de Sfax, Tunisie

C.R.D.A (2015) Exploitation de la nappe profonde en 2014. Annuaires d'exploitation des nappes aquifères de Sfax. Commissariat Régionale d'Activité Agricole de Sfax, Tunisie

Edmunds WM, Tyler SW (2002) Unsaturated zones as archives of past climates: toward a news proxy for continental regions. J Hydrogeol 10:216–228

Edmunds WM, Guendouz AH, Mamou A, Moula A, Shand P, Zouari K (2003) Groundwater evolution in the Continental Intercalaire aquifer of southern Algeria and Tunisia: trace element and isotopic indicators. Appl Geochem 18:805–822

El Batti, Andrieux (1977) Etude hydrogéologique et géophysique du secteur Wadrane. Rapport interne

Fairbanks RG (1989) A 17000 year glacio-eustatic sea level record: influence of glacial melting rates on the Younger Dryas event anddeep-ocean circulation. Nature 342:367–642

Fedrigoni L, Krimissa M, Zouari K, Maliki A, Zuppi GM (2001) Origine de la minéralisation et comportement hydrogéochimique d'une nappe phréatique soumise a' des contraintes naturelles et anthropiques sévères: exemple de la nappe de Djebeniana (Tunisie). Earth Planet Sci Lett 332:665–671

Gassara A, Ben Marzouk A (2009) Hydrogéologie de la nappe semi-profonde de Sfax. Rapport de CRDA de Sfax, Tunisie

Gay D (2004) Fonctionnement et Bilan de Retenues Artificielles en Tunisie: Approche Hydrochimique et Isotopique. PhD Thesis, University of Paris XI, France

Geyh MA (2000) An overview of ^{14}C analysis in the study of the groundwater. Radiocarbon 42(1):99–114

Gonfiantini R (1986) Environmental isotopes in lake studies. In: Fritz P, Ch. Fontes J (eds) Handbook of environmental isotope geochemistry, the terrestrial environment B, vol 2, Amsterdam, pp 13–163

Hajjem A (1980) Etude hydrogéologique de la région de Sidi Abid. Rapport interne. Direction des Ressources en Eaux de Sfax, Tunis

Hchaichi Z (2008) Etude hydrogéologique et géochimique de la nappe intermédiaire de Sfax et sa relation avec le système phréatique du bassin Nord de Sfax. Mémoire de Mastère, Ecole Nationale d'Ingénieurs de Sfax (ENIS), Tunisie

Hchaichi Z, Abid K, Zouari K (2013) Use of hydrochemistry and environmental isotopes for assessment of groundwater resources in the middle aquifer of the Sfax basin (Southern Tunisia). J Carbonates Evaporites. doi:10.1007/s13146-013-0165-2

I.N.M (2011) Données météorologiques. Institut National de la Météorologie de Sfax, Tunisie

Kamel S (2010) Recharge of the plio-quaternary water table aquifer in Tunisian chotts region estimated from stable isotopes. Environ Earth Sci 63:189–199

Kamel S, Younes H, Chkir N, Zouari K (2008) The hydrogeochemical characterization of ground waters in Tunisian Chott's region. Environ Geol 54:843–854

Lis G, Wassenaar LI, Hendry MJ (2008) High-precision laser spectroscopy D/H and $^{18}O/^{16}O$ measurements of microliter natural water samples. Anal Chem 80:287–293

Ma J, Ding Z, Edmunds WM, Gates JB, Huang T (2009) Limits to recharge of groundwater from Tibetan plateau to the Gobi desert, implications for water management in the mountain front. J Hydrol 364:128–141

Maliki MA (2000) Etude hydrogéologique, hydrochimique et isotopique du système aquifère de Sfax (Tunisie). Thèse Doctorat. Univ. de Tunis II, Tunis

Maliki MA, Krimissa M, Michelot JL, Zouari K (2000) Relation entre nappes superficielles et aquifère profond dans le bassin de Sfax (Tunisie). Earth Planet Sci 331:1–6

Mazor E (1991) Applied chemical and isotopic groundwater hydrology. Open University Press, Buckingham, p 282

Rozanski K, Araguas-Araguas L, Gonfiantini R (1993) Isotopic patters in modern global precipitation. In: Swart PK et al (eds) Climate change in continental isotopic records. Geophysical Monograph Series, vol 78. AGU, Washington DC, pp 1–36

Scanlon BR, Keeze KE, Flint AL, Flint LE, Gaye CB, Edmunds WM, Simmers I (2006) Global synthesis of groundwater recharge in semiarid and arid regions. Hydrol Process 20:3335–3370

Takrouni M, Michelot JL, Maliki A, Zouari K (2003) Relation entre aquifère profond, nappes superficielles et intrusion marine dans le Bassin de Sfax (Tunisie). Hydrol Mediterr Semiarid Regions 278:1–7

Tayech B (1984) Etudes palynologiques dans le Néogène du Cap Bon (Tunisie). Thèse de Doctorat, Univ. Claude Bernard, Lyon I

Taylor CB (1976) IAEA isotope hydrology laboratory, technical procedure note no. 19. International Atomic Energy Agency, Vienna

Tijani MN, Loehnert EP, Uma KO (1996) Origin of saline groundwaters in the Ogoja area, Lower Benue Trough, Nigeria. J Afr Earth Sci 23:237–252

Trabelsi R (2008) Contribution à l'etude de la salinisation des nappes phrèatiques côtières. Cas du système de Sfax-Mahdia. Thèse Doctorat, Faculté des Sciences de Sfax, Tunisia, p 175

Trabelsi R, Zaïri M, Smida H, Ben Dhia H (2005) Salinisation des nappes côtières: cas de la nappe nord du Sahel de Sfax, Tunisie. C R Acad Sci Paris 337:515–524

Trabelsi N, Zaïri M, Triki I, Ben Dhia H (2006) Contribution d'un SIG à la gestion des ressources en eaux souterraines: Cas de la nappe profonde de Sfax, Tunisie, Conférence francophone ESRI. Issy les moulineaux 2006:1–7

Yangui H, Zouari K, Trabelsi R, Rozanski K (2010) Recharge mode and mineralization of groundwater in a semi-arid region: Sidi Bouzid Plain (central Tunisia). J Environ Earth Sci 63:969–979

Zebidi H (1989) Hydrogéologie de la nappe profonde de Sfax. Rapport interne. DGRE de Tunis

Zouari K, Chkir N, Ouda B (2003) Palaeoclimatic variation in Maknassi basin (central Tunisia) during Holocene period using pluridisciplinary approaches. IAEA, Vienna, CN 80-28